

Document downloaded from:

<http://hdl.handle.net/10251/165730>

This paper must be cited as:

Mesado, C.; Miró Herrero, R.; Verdú Martín, GJ. (2020). Methodology for neutronic uncertainty propagation and application to a UAM-LWR benchmark. *Progress in Nuclear Energy*. 126:1-12. <https://doi.org/10.1016/j.pnucene.2020.103389>



The final publication is available at

<https://doi.org/10.1016/j.pnucene.2020.103389>

Copyright Elsevier

Additional Information

Methodology for neutronic uncertainty propagation and application to a UAM-LWR benchmark

C. Mesado, R. Miró, G. Verdú*

*Institute for the Industrial, Radiophysical and Environmental Safety (ISIRYM)
Universitat Politècnica de València
46022 Valencia, Spain*

Abstract

This work covers an important point of the benchmark released by the expert group on Uncertainty Analysis in Modeling of Light Water Reactors (UAM-LWR). This ambitious benchmark aims to determine the uncertainty in LWR systems and processes in all stages of calculation, with emphasis on multi-physics (coupled) and multi-scale simulations. Specifically, in this work, a simplified BWR core is used to propagate the uncertainty of nuclear data. [Due to a high computational cost in the analysis all fuel assemblies are modeled as fresh.](#) The propagation is subdivided into two levels i) assembly level –with SCALE6.2.1 and SAMPLER module–, and ii) core level, –with PARCSv3.2 and DAKOTA 6.3–. The first level takes into account the uncertainties contained in the master library ENDF/B-VII.1 and as a result a problem-dependent neutronic library in NEMTAB format is obtained using TXT2NTAB code. This is a friendly MATLAB code developed within this work. Finally, the uncertainty contained in the neutronic library is further propagated through PARCS. A different approach is presented in this work to propagate the uncertainty between codes. Following this approach only two neutronic libraries are generated, one with the average responses and the other with their standard deviations. Then, the standard deviation and a matrix of perturbation factors are used to perturb the main neutronic parameters. [A parallel work is done to propagate the thermal-hydraulic parameters in a PWR core \[1\]](#)

Keywords: U&S analysis, uncertainty propagation, 3D core model, SCALE6.2, SAMPLER, PARCS, TXT2NTAB

1. Introduction

This work covers the main phases of the benchmark released by the expert group on *Uncertainty Analysis in Modeling of Light Water Reactors* (UAM-LWR). The UAM benchmark [2] was conceived in 2006 at the University of Pisa (Italy) due to the need of best estimate calculations together with its confidence bounds. Thus, the UAM expert group pretends to obtain the current state and future needs of *Uncertainty and Sensitivity* (U&S) analysis in modeling, with emphasis on multi-physics (coupled) and multi-scale simulations. With this information, the benchmark main goal is to determine the uncertainty in LWR systems in all stages of calculation. The benchmark is subdivided into three phases:

1. Neutronic phase: multi-group microscopic and macroscopic cross-section library and criticality analyses.
2. Core phase: stand-alone thermal-hydraulic and neutronic codes.
3. System phase: coupled thermal-hydraulic and neutronic code.

To establish proper confidence bounds an *Uncertainty Quantification* (UQ) method must be used. [There are several UQ methods, for example \[3\] compares several methods for uncertainty propagation and \[4\] uses the SHARK-X methodology to propagate nuclear data uncertainties in CASMO-5.](#) However, one of the most used method in the nuclear field, and also recommended by the UAM benchmark organizers, is the *Gesellschaft für Anlagen und Reaktorsicherheit* (GRS). The GRS method is widely used in the literature, for example [5]. [The main advantages of GRS are that it is easy to implement and it is based on existing covariances, the downsides are that each input parameter must have a pre-defined *Probability Distribution Function* \(PDF\) to quantify its uncertainty and that it is limited to the existing covariances –no thermal scattering and no clear fission yield correlations for example–.](#) When using the GRS methodology, the user must be aware of a few things:

1. A range and a PDF for each uncertain input parameter must be identified. Ideally, the PDFs should be obtained using experimental data, [for example \[6\]](#). However, in reality such data is commonly not available. In such cases, it is common to assign a uniform or normal distribution [7], otherwise expert judgment is used to assign a range and PDF. Nevertheless, the use of expert judgment is often unreal and should be used with caution.
2. The uncertain input parameters are sampled n times, there

*Corresponding author

Email address: gverdu@iqn.upv.es (G. Verdú)

are several sampling techniques that can be used. Being the most common the *Simple Random Sampling* (SRS) –expensive method since the n must be high compared to other methods to obtain the same coverage–, *Stratified Sampling* with a better coverage and *Latin Hypercube Sampling* (LHS) with an improvement over the stratified sampling with additional computational cost to reduce the bias. It is known that more accurate model response variance is obtained using LHS [8], but results differences are not significant [9].

3. Parametric or non-parametric samplings are possible to obtain the number of samples or code runs, n . Parametric samplings assume a statistical distributions in the sampled data. Thus, this distribution must be tested so that the sampling is reliable. Whereas any statistical distribution can be assumed in non-parametric samplings. The number of samples could be greatly reduced using a non-parametric sampling because all uncertain parameters are sampled at the same time. Therefore, with non-parametric sampling, the number of runs depends only on the tolerance and confidence interval of responses. That implies that the number of input parameters involved do not have any limitation. It is also important to check the convergence of the parameters of interest (means, standard deviation, skewness...) as a function of n .

The determination of the minimum sample runs, n , is important. For a non-parametric approach, the parameter n is such that when the code is run n times –or samples–, the response of interest will meet a certain tolerance limit (required a priori). The method to obtain n with a certain uncertainty, α , and a statistical confidence, β , was developed by Wilks ([10] and [11]). The formula for one-sided tolerance region ($s = 1$) is given by Eq 1 and Eq 2 for first and second order (k) respectively. For example, for a one-sided 95/95 tolerance region, a minimum sample size of 59 is obtained if $k = 1$, but the sample size increases to 93 if $k = 2$. The same sample size (93) is obtained if $k = 1$, but a two-sided 95/95 tolerance region is specified (as suggested in [12]). However, in a recent study ([13] and [14]) the recommended minimum sample size for the same conditions ($k = 1$ and two-sided) increases to 146 according to Eq 3, where ${}_nC_j$ is the number of combinations of n items taken j at a time. Finally, if there are several dependent responses (r), the minimum sample size increases as given in Eq 4 for $k = 1$, see [15] and [16]. For three dependent responses, one-sided 95/95 tolerance region and $k = 1$, the sample size is 124. More information to determine the minimum sample size can be found in [17].

$$1 - \alpha^n \geq \beta \quad (1)$$

$$1 - \alpha^n - n(1 - \alpha)\alpha^{(n-1)} \geq \beta \quad (2)$$

$$1 + \alpha^n - 2\alpha^n \sum_{j=0}^n {}nC_j \left(\frac{1 - \alpha}{2\alpha}\right)^j \geq \beta \quad (3)$$

$$\sum_{j=0}^{n-s-r} {}nC_j \alpha^j (1 - \alpha)^{(n-j)} \geq \beta \quad (4)$$

4. High-fidelity model vs surrogate model. For complex models, if a high fidelity model is used to propagate the uncertainty, the computational effort could be prohibitive. In this case, the high-fidelity or full model can be replaced by a surrogate model. The surrogate model represents the same physical scenarios but it runs simulations faster at expenses of accuracy and range of applicability.

GRS makes use of a non-parametric sampling, the high-fidelity model and the Wilks' formula to obtain n . The U&S analysis can be obtained with any statistical software available in the market, for example SAMPLER or DAKOTA. The former is included in SCALE6.2 and the latter is developed at Sandia National Laboratory. Both of them are able to perform UQ (average responses, standard deviations, confidence intervals...). In addition to this information, DAKOTA calculates *Sensitivity Analysis* (SA) by means of sensitivity coefficients assuming linear –*Simple Correlation Coefficient* (SCC) and *Partial Correlation Coefficient* (PCC)– and non-linear relationships –*Spearman's Rank Correlation Coefficient* (SRCC) and *Partial Rank Correlation Coefficient* (PRCC). One of the easiest way to extract correlation coefficients is with PRCC. It has the advantage that can capture non-linear correlations between two parameters while holding all the other parameters constant. In this work, PRCC is used to assess SA. Unfortunately, SAMPLER is not able to perform SA yet. Several examples using this coefficient can be found in the literature, for example [18] and [7]. More information can be found in [19].

1.1. Overview

This paper presents a methodology to propagate the uncertainty of nuclear data and has been divided into six sections. The current section introduces the UAM benchmark and GRS methodology. The second section gives an explanation of models used in this work. The third section shows the process to obtain a problem-dependent neutronic library. Section 4 details the methodology for the uncertainty propagation. The fifth section shows the results for the uncertainty propagation of nuclear parameters at lattice and core level. Finally, the last section, states, briefly, the conclusions.

Three comments are worth to mention here. First, even though the methodology is shown without thermal-hydraulic coupling, there is not any limitation that prevents it to be coupled with a thermal-hydraulic code, as it was proved in [7] and [20]. Second, due to the high number of data generated in this work, only the most representative results are shown in this paper which intends to show the possibilities that the methodology presents. The reader is referred to [21] to obtain the complete spectrum of results. Third, in this work thermal-hydraulic parameters are not included because there is not thermal-hydraulic coupling. However, a parallel work is done to propagate the thermal-hydraulic parameters in a PWR core [1] (without neutronic propagation)

145 2. Models

Two different models are developed in this work: lattice and core model. Regarding the lattice model, SCALE6.2.1 code is used with TRITON/NEWT module to produce problem-dependent cross sections in a BWR. The core model is build using PARCSv3.2 code without thermal-hydraulic feedback. SCALE model makes use of the new v7-56 master cross section library. It is known that higher predictions can be obtained with the finer v7-252 library, however, due to the high number of samples, the v7-56 library is used in this work to reduce computational time. As a result, homogenized and collapsed problem-dependent cross sections are obtained. The verification of the lattice model is made comparing the predicted macroscopic cross sections and CASMO-4 results [21]. It must be said that scripts are programmed to automatically generate the correspondent models using MATLAB, see [21]. Therefore, it is easy to produce input decks with the confidence that they are already tested.

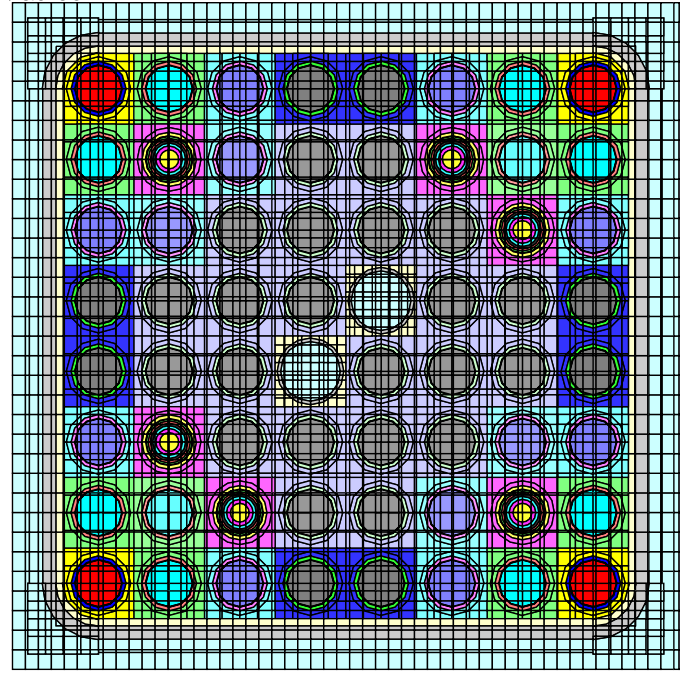


Figure 1: SCALE model for a BWR assembly.

2.1. Lattice model

Figure 1 shows an example of a BWR lattice model without control rods. Most BWR cores contain burnable absorber pins, these pins provide an effective mean to control the core power as they insert negative reactivity while they are burning. According to [22], three different recommendations are followed to model these pins.

- Due to their fast burn-up behavior, they are modeled using different concentric rings. An example is seen in the central pin of Figure 2. The use of different geometrical bodies helps to obtain an improved flux and isotopic radial distribution.
- The cell treatment –when multigroup libraries are used– is performed specifying the multiregion cell option. This option is preferred when the default cell treatment (lattice) is not appropriate. With multiregion, several concentric rings can be specified, and thus, the geometric approximation in previous recommendation is followed.
- Burnable absorber pins are depleted using constant flux instead of constant power. Again, due to its fast depletion, this helps to obtain a better isotopic prediction.

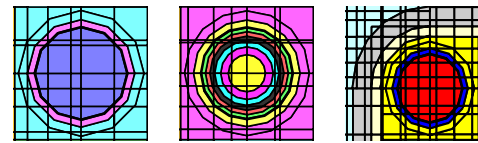


Figure 2: From left to right, details for a fuel pin, burnable absorber pin and fuel assembly corner.

Even though the use of accurate Dancoff factors is recommended for very heterogeneous models –such as BWR–, the default Dancoff factors calculated by SCALE –assuming an infinite lattice of equal fuel pins– are used in this model due to the memory required and the computational time.

The main features for the lattice physics model are summarized in Table 1. In order to perform a verification of this model, a code-to-code comparison between SCALE (red lines) and CASMO-4 (black lines) as reference code is shown in Figure 3. The comparison is made for the whole void range, control rods withdrawn and a fuel temperature equal to 879.5 K. For a full comparison the reader is redirected to [21]. The same trends can be seen in [23].

2.2. Core model

A BWR is build with PARCS as a core model, its main characteristics are summarized in Table 2. It is important to note that all fuel assemblies are fresh, thus, simplifying the segments and the calculation time. The model contains 2 prompt neutron groups and 6 delayed neutron groups. All boundary conditions are set to zero flux, thus all neutrons traveling outside the reflector are lost. The decay heat model is activated and the diffusion equation solver is HYBRID

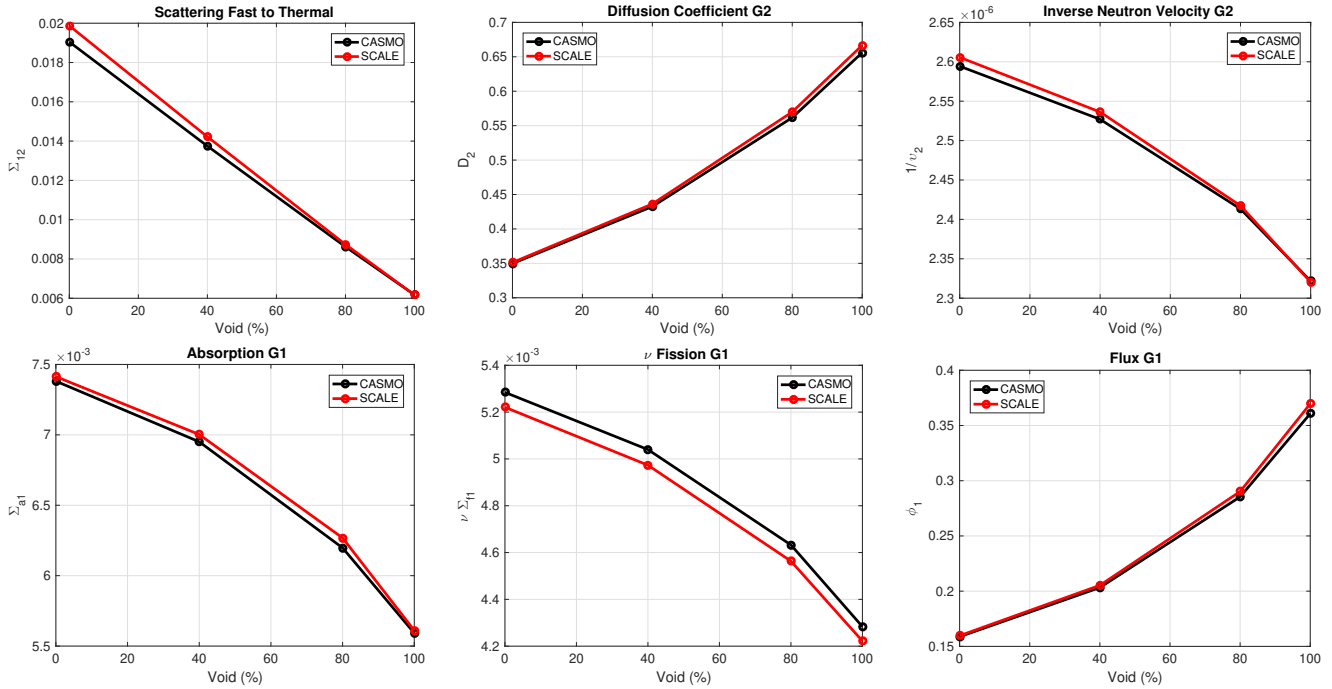


Figure 3: Lattice model verification – code-to-code comparison between CASMO-4 and SCALE6.2.

Property	Value
Number of segments	9
Cross section library	v7-56
Cross section processor	CENTRM
Parameter addnux	4
Energy groups	40 & 16
Energy boundary	0.625 eV
Pin cell discretization	4x4
Fuel pin treatment	Latticecell
Burnable pin treatment	Multiregion
Operation conditions	Fresh
Rings in Gd-pins	6
Dancoff factors	Default
Feedback points $T_{fuel} \times \rho_{mod}$	7x5

Table 1: Main features for the lattice physics model.

Property	Value
Power level	92%
Fuel assemblies	624
Assembly layout	8x8
Control rod banks	4
Radial cells	30x30
Axial cells	27 (2 refl.)
Cell dim. (cm)	15.24x15.24
Cell height(cm)	15.24
Fuel cells	624
Reflector cells	116
Fuel types	4
Neutronic comp.	103 (3 refl.)

Table 2: Main features for the core physics model.

–recommended in PARCS manual–. The association between fuel assemblies and neutronic nodes is one to one, thus the models are not collapsed. The thermal-hydraulic 3D boundary conditions used are between 600 K and 1200 K for the fuel temperature, and moderator density between 100 kg/m³ and 800 kg/m³. These are given to PARCS as 3D radial maps. The fuel type mapping and the control rod bank distribution are seen in Figure 4.

3. NEMTAB library generation

Regarding the lattice model, it is important to know the segment information related to the core in question. If the whole core is discretized in cells –with length of 15.24 cm on

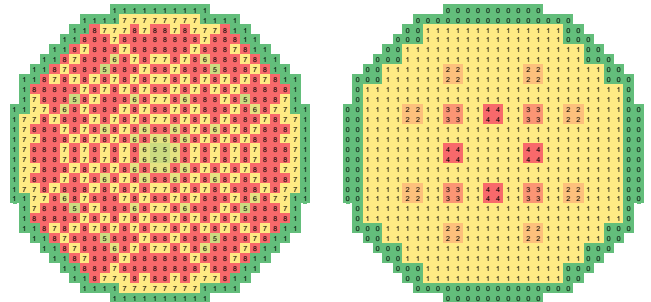


Figure 4: Fuel type radial mapping (left) and control rod bank distribution (right).

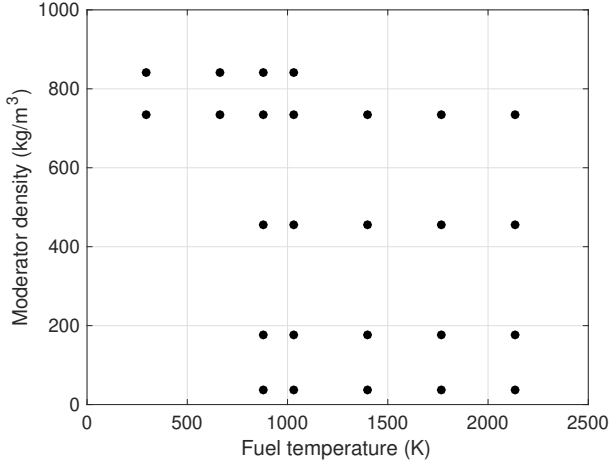


Figure 5: Feedback parameters combinations.

all sides–, a segment lumps all cells that have similar neutronic²⁶⁵ behavior, i.e. cells that have similar composition and reactor history. This approach allows a reduction of lattice simulations and thus, a computational time improvement. Then, an expert user must decide the feedback state points for each feedback parameter. This decision has strong implications in²⁷⁰ the neutronic code results. In this work, 52 different feedback combinations are studied for each segment: 5 moderator densities –or a combination of void fractions and moderator temperature–, 7 fuel temperatures and 2 control rod states (in²⁷⁵ and out) as seen in Table 3 and Table 4. The reactor history points are constant and can be seen in the same tables, except the control rod history which is always out. Nonetheless, some of these feedback combinations are not realistic, i.e.²⁸⁰ when both, moderator density and fuel temperature, are either very high or very low. Thus, the non-realistic combinations are removed and the chosen feedback combinations in this work can be seen in Figure 5. The segments representing the reflector do not require simulations with control rods in, thus they have half of the feedback state points (26).²⁸⁵

Some comments related to the chosen feedback state points are needed here. The fuel temperature range (293 K to 2132.2 K) is broad enough to cover almost all possible design base²⁹⁰ accidents, higher temperatures could lead to fuel damage or even melting. Regarding the moderator, the selected feedback²⁹⁵

	T_{fuel} (K)
1	293.0
2	660.8
3	879.5
4	1028.6
5	1396.5
6	1764.3
7	2132.2
Hist.	879.5

Table 3: Fuel temperature feedback and history points.

parameters in the moderator range from pure liquid and up to 100% steam, several intermediate points are included where both phases coexist at saturated temperature. In a real problem,²⁵⁰ more intermediate points could be needed, especially inside the zone of normal operation for a BWR, i.e. moderator density 400–800 kg/m³ and fuel temperature between 400 K and 1400 K. If a real problem is known to develop with high voids,²⁵⁵ then the void fraction points should be focused in the region greater than 80%. Two reasons apply here: (i) predictions in this region are known to be less accurate and (ii) neutronic parameters have a stronger variation in this range. Both reasons are reassured in [23]. However, the points and ranges defined in Table 4 are enough for the purpose of this work: develop and test the methodology in an arbitrary case.²⁶⁰

Generated NEMTAB libraries contain tabulated cross sections for three different feedback parameters, i.e. fuel temperature, moderator density and control rod state (boron concentration is not yet considered). Control rod dependence is handled creating two different NEMTAB libraries, one for rodded conditions (NEMTABR) and one for unrodded conditions (NEMTAB). The problem-dependent cross section library generated is only valid for this particular BWR and for specific operation conditions (matching the reactor history and burn-up), in this case fresh compositions. NEMTAB library contain the neutronic parameter information tabulated for each neutronic composition –or cells with identical neutronic behavior–. Since it is assumed that neutronic compositions for reflector segments are not significantly affected by control rods, the data for reflector compositions is invariable for both libraries.

In this work the NEMTAB libraries are generated for fresh conditions only due to high computational resources needed. This is accomplished setting a low burn-up level and only one short cycle in the SCALE model. However, the methodology is not limited to fresh conditions and any burn-up can be used. To obtain neutronic libraries for a specific burn-up, the neutronic parameters are the result of an interpolation of the predicted neutronic parameters as a function of burn-up. The correspondent burn-up for each neutronic cell, the operation conditions and the information related to the segments (core configuration) is given by the nuclear power plant. The neutronic compositions in the generated NEMTAB library are filled according to this information. According to the segment information, there are 4 fuel assembly types and 9 segments (3

	ρ_{mod} (kg/m ³)	Void (%)	T_{mod} (K)
1	38.14	100	561.4
2	177.53	80	561.4
3	456.32	40	561.4
4	735.11	0	561.4
5	840.34	0	493.0
Hist.	456.32	40	561.4

Table 4: Moderator feedback and history points.

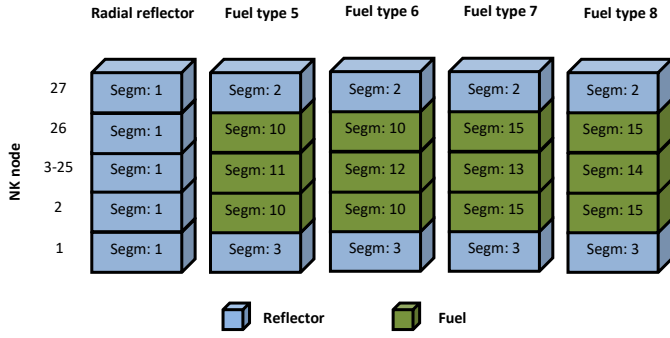


Figure 6: Segment composition for each fuel type.

of them are reflector zones), see Figure 6.

A neutronic composition is defined for each axial level and fuel assembly type. This results in smaller neutronic libraries, but can only be used in fresh conditions or very low burn-up levels. If the reactor height is divided into 27 axial levels (n_z) – being the upper and lower levels non-active – and there are 4 different fuel bundle types (n_{type} , see Table 2), the total number of neutronic compositions NK_{comp} is 103 according to Eq 5. However, three of these neutronic compositions are used to simulate reflector cells (top, bottom and radial).

$$NK_{comp} = n_{type}(n_z - 2) + n_{refl} = 4(27 - 2) + 3 = 103 \quad (5)$$

A MATLAB program, TXT2NTAB code, is developed to automate this process and generate NEMTAB libraries out of SCALE results, see [24]. Besides, a graphical and user-friendly GUI is provided with TXT2NTAB.

4. Methodology

A methodology is devised to propagate neutronic uncertainties through SCALE6.2 and PARCSv3.2. The propagation process can be divided into two steps. The first step performs the propagation at assembly level with SCALE, while the second step is at core level with PARCS. The first level makes use of the new SAMPLER module to perturb –with the default perturbation library– and propagate the uncertainty of nuclear data contained in the master library ENDF/B-VII.1 (default in SCALE6.2). SCALE can predict neutronic parameters to be used in a core physics code. To achieve this, a MATLAB program –TXT2NTAB– is developed to translate SCALE results to neutronic libraries in NEMTAB format. TXT2NTAB is also able to obtain NEMTAB libraries with uncertainty information and the user can interact either with the developed GUI or with an ASCII interface. In the second level, the uncertainty contained in this neutronic library is further propagated through PARCS code. PARCS source code is modified to perturb the main cross sections using the standard deviation values and a set of perturbation factors generated with DAKOTA 6.3 statistical tool. However, this process could be done externally to PARCS without the need to modify the source code. Finally, the uncertainty

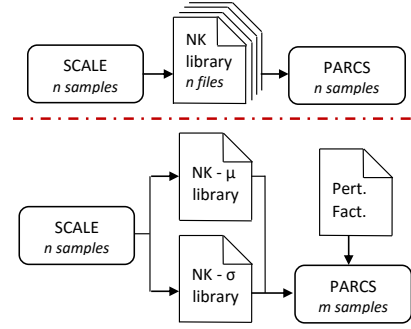


Figure 7: Flow diagram to propagate uncertainty between codes (two options).

propagated is reflected in PARCS output parameters (multiplication factor $-k_{eff}-$, axial power peak $-P_z-$ and peak node location $-N_z-$). The latter being the axial node index where the maximum value of the axial power distribution is found.

4.1. Discussion

One of the decisive points in the propagation methodology is the uncertainty propagation between codes, SCALE-PARCS in this case. In fact, this is still a point of discussion in the UAM benchmark. An example of a full propagation is presented in [4]. Two options arise here.

- The propagation is done creating as many neutronic libraries for the core physics code as samples in the lattice physics code. Then, the core physics code is run several times with a different neutronic library each time. This option is widely used in the literature, for example [25], and is sketched in the upper side of Figure 7.
- Nonetheless, in this work, a new approach is presented. Only two neutronic libraries are created, one with the average responses and the other with standard deviations. Then, the core physics code is run several times, each time perturbing the neutronic parameters (average responses) with the standard deviation values and a matrix of perturbation factors that are previously generated. This option is sketched in the lower side of Figure 7.

Some differences are identified for each option.

- While the implementation of the first option is straightforward, some work needs to be done for the second option (generate neutronic libraries with average and standard deviation values, generate the matrix of perturbation factors and perturb neutronic parameters either internally or externally to the core physics code).
- The sample size for both codes –lattice and core– must be the same in the first option. However, sample sizes are independent in the second option.
- The core physics code interpolates neutronic parameters according to the nodal feedback parameters –given by the user or a thermal-hydraulic code–. This action implies an

uncertainty interpolation in the first option. Since the accuracy of the interpolation is dependent on the distance to the fixed points, it implies some error in the uncertainty propagation. This is not a problem in the second option since it propagates the uncertainty using the standard deviation and a perturbation factor.

- No distribution assumption is made in the first option. In the second option, normality must be assumed for the neutronic parameters in order to use their standard deviations. This assumption must be checked afterwards with a normality test.

The second option is followed in this work and its methodology is explained in detail in the following subsections, the most important data is summarized in Table 5. Before going into details on the developed methodologies, a comment regarding the chosen sample size must be made.

- Lattice level. The uncertainty through SCALE is propagated using the covariance library included with SAMPLER. Therefore, the accuracy of results increases with the number of samples. The maximum number of samples allowed in SAMPLER is chosen, that is 1000 samples or perturbations.
- Core level. There are 3 dependent output parameters (k_{eff} , P_z and N_z) and only their upper tolerance region is of interest. Thus, as it was explained in Section 1, for a 95/95 case with one-sided tolerance region and 3 partially dependent responses, the minimum sample size is 124, see Eq 4. Nevertheless, 1000 samples are run again even though the sample size for the lattice and core physics codes are independent.

4.2. Lattice level

SAMPLER module is used to propagate the uncertainty. This module applies the perturbations –found in the perturbation library– to the nuclear data found in the master library ENDF/B-VII.1. It must be said that fission yields and decay data are not perturbed since their uncertainty information is still not accurate. In this case, the whole core is composed by 9 different segments, see Figure 6. Each segment must be run 1001 times (one per perturbation set plus one non-perturbed case). Due to the high number of simulations ($9 \cdot 1001 = 9009$) and computational resources, the analysis is performed only at fresh conditions i.e. the lattice model is not depleted. The whole process can be seen in Figure 8.

Seven problem-dependent homogenized and collapsed cross sections are defined as output parameters in SAMPLER. These are obtained for each feedback parameter combination in SCALE –see Section 3– and for each segment. The responses are listed next.

1. Diffusion coefficient for fast group, D_1 .
2. Diffusion coefficient for thermal group, D_2 .

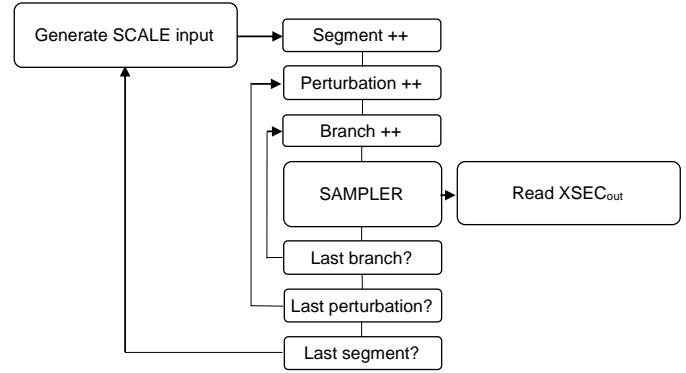


Figure 8: Flow diagram to generate homogenized and collapsed cross sections.

3. Absorption cross section for fast group, Σ_{a1} .
4. Absorption cross section for thermal group, Σ_{a2} .
5. Average neutrons per fission times production cross section for fast group, $\nu\Sigma_{f1}$.
6. Average neutrons per fission times production cross section for thermal group, $\nu\Sigma_{f2}$.
7. Scattering cross section from fast to thermal group, Σ_{12} (down-scattering).

4.3. Core level

Five main steps are followed to propagate the uncertainty through PARCS. The BWR core model detailed in Section 2.2 is used.

1. The results of SAMPLER calculations are gathered for each segment. Especially important are the average responses –over all samples or perturbations– and its standard deviations.
2. Two problem-dependent NEMTAB libraries are generated with TXT2NTAB and according to Section 3. One containing the average cross sections and the other their standard deviations. The average and standard deviations for the seven main cross sections are obtained in the previous step, all other cross sections and kinetic parameters are obtained from the unperturbed simulation. Values in this library are the result of an interpolation of each neutronic parameter for a certain burn-up level, as explained in Section 3. In this work, the value at zero burn-up is always used because the lattice model is simulated at fresh conditions.
3. Using DAKOTA, 1000 sets of perturbations are generated for the seven main cross sections and each neutronic composition. At this point of the developed methodology, and as a simplification, the correlations for main cross sections and neutronic compositions are not taken into account for sampling. Nonetheless, this needs to be covered in a future work, along with a more realistic case. According to Eq 5, there are 103 neutronic compositions, each

Property	Lattice model	Core model
Code	SCALE6.2.1/NEWT	PARCSv3.2
U&S code	SAMPLER	DAKOTA 6.3
Model description	Section 2.1	Section 2.2
Simulation state	SSA (fresh)	SSA
Input parameters	Problem-independent cross sections in ENDF/B-VII.	Problem-dependent cross sections, whole core and all feedback param. combinations.
Num. input param.	99232	715
Output parameters	Problem-dependent cross sections for one segment and specific feedback parameter set.	Multiplication factor, axial power peak and peak node location.
Num. output param.	7	3
Sampling method	SRS	SRS

Table 5: Data summary for cross section parameter uncertainty propagation.

with seven main cross sections. However, three neutronic compositions represent reflector zones and have only five main cross sections since both fission cross sections are not perturbed. Therefore, the number of input parameters is $100 \cdot 7 + 3 \cdot 5 = 715$. Note that perturbation factors are not defined for each feedback parameter (fuel temperature, moderator density and control rod) or collapsed energy group. All perturbations are generated with the following properties: normal PDFs, random sampling method, 0 as average value and an upper/lower limit of ± 1 , see Eq 6.

- Then, 1000 steady state simulations with PARCS (without thermal-hydraulic coupling) are run, each simulation with a different set of perturbations. PARCS source code is modified to read the perturbations generated by DAKOTA and the NEMTAB library of standard deviations. Therefore, PARCS is able to perturb the main cross sections, according to the following formula:

$$XS_i^p = \bar{X}S_i + \sigma_{XS_i}Q_i \quad (6)$$

Where

i is the perturbation index (up to 1000),

XS_i^p is a vector containing all 715 perturbed cross sections,

$\bar{X}S_i$ is a vector containing all averaged cross sections, these are read by default by PARCS from the NEMTAB library of average values,

σ_{XS_i} is a vector containing all cross section standard deviations, these are read by PARCS from the NEMTAB library of standard deviation values, and

Q_i is a vector containing all perturbation factors generated with DAKOTA for set i .

- Finally, the U&S analysis is performed with DAKOTA. The output parameters are defined as the multiplication factor $-k_{eff}-$, the axial power peak $-P_z-$ and peak node

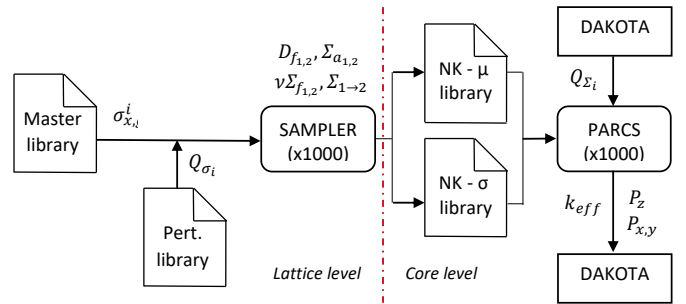


Figure 9: Flow diagram for neutronic data propagation.

location $-N_z-$ predicted by PARCS. These output parameters are chosen because they are inherent to the reactor safety. With the responses and perturbation factors, DAKOTA is able to perform a complete U&S analysis.

Figure 9 shows a flow diagram for the neutronic data propagation methodology at lattice and core level.

5. Results

As stated in Section 1 and due to the high number of data generated in this work, only the most representative results are shown in this paper which intends to show the different possibilities of the methodology. The reader is referred to [21] to obtain the complete spectrum of results. This section is split in subsections according to each level (lattice and core).

5.1. Lattice level

The uncertainty information is obtained for the main homogenized cross sections (D_1 , D_2 , Σ_{a1} , Σ_{a2} , $\nu\Sigma_{f1}$, $\nu\Sigma_{f2}$ and Σ_{12}), each feedback parameter combination and each segment in the core. Thus, there are a lot of data to process. For sake of brevity, only the most representative results are presented here. Results for other segments are very similar. Reflector segments are more dissimilar because they use different homogenized

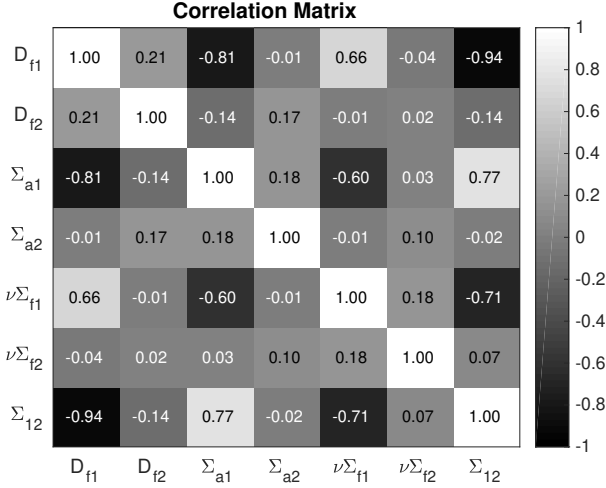


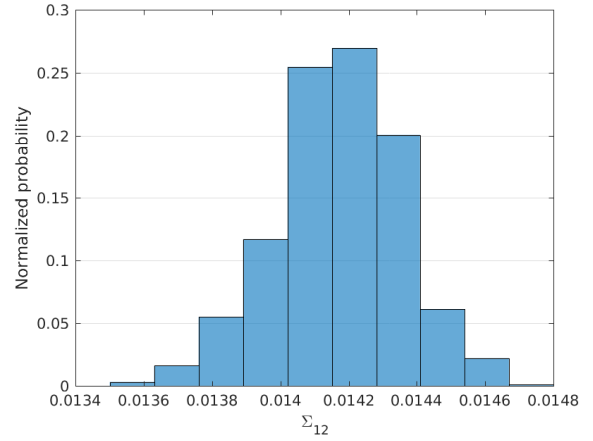
Figure 10: Correlation matrix among output parameters in a representative segment and branch.

materials.

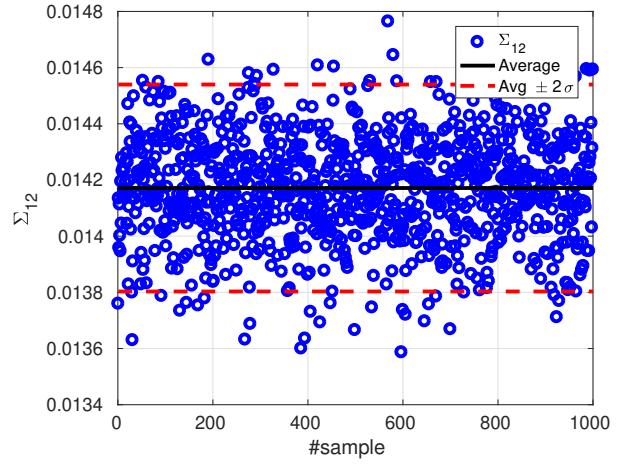
Figure 10 shows the correlation matrix between output parameters (homogenized and collapsed cross sections) for fuel segments. These results correspond to a representative segment (14) and branch with fuel temperature of 853.50 K, moderator temperature of 561.40 K and 0.45632 g/cm³ as moderator density. For fuel segments, the most correlated output parameters are 1) $D_1 - \Sigma_{12}$ with a very strong negative correlation ($|r| \geq 0.8$), 2) $D_1 - \Sigma_{a1}$ with a very strong negative correlation and 3) $\Sigma_{a1} - \Sigma_{12}$ with a strong positive correlation ($0.6 \leq |r| < 0.8$). For reflector segments the most correlated output variables are 1) $D_1 - \Sigma_{12}$ with a very strong negative correlation and 2) $\Sigma_{a1} - \Sigma_{a2}$ with a moderate positive correlation ($0.4 \leq |r| < 0.6$). Comparing the results for a case with and without control rods, it is seen that some correlations increase significantly, these are 1) $\Sigma_{a1} - \Sigma_{12}$, 2) $\Sigma_{a1} - D_1$ and 3) $\Sigma_{a1} - \nu\Sigma_{f1}$. In these cases, correlations become stronger, towards the positive or the negative side. Almost all other correlations are weak ($0.2 \leq |r| < 0.4$) or very weak ($|r| < 0.2$).

For example, the information for scattering cross section is shown in Figure 11 (histogram, scatter plot and moving average). This figure is obtained for the same segment and branch as Figure 10. Histograms are useful to assign a distribution to parameters, for example normality. Scatter plots are good to visualize the point clouds distribution resulting from all samples and determine how many samples are outside the 2σ boundaries. Finally, the moving averages can be used to determine the parameter convergence, the higher the number of samples, the higher the convergence. It is seen that the moving averages converge, roughly, at 300 samples.

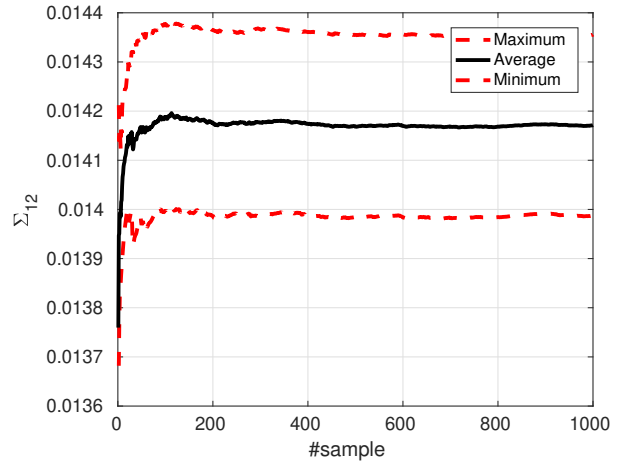
The Lilliefors tests for normality is performed for the homogenized cross sections and the resulting p-value¹ can be



(a) Histogram.



(b) Scatter plot.



(c) Moving average.

Figure 11: Results for scattering cross section in a representative segment and branch.

¹A small p-value (typically < 0.05) indicates strong evidence to reject the

	Average	Std. Dev.	p-value
D_1	1.540	3.66E-2	0.05
D_2	3.58E-1	1.03E-3	0.62
Σ_{a1}	5.90E-3	5.02E-5	0.52
Σ_{a2}	2.77E-2	1.50E-4	0.44
$\nu\Sigma_{f1}$	2.70E-3	7.48E-5	0.38
$\nu\Sigma_{f1}$	2.69E-2	1.41E-4	0.85
Σ_{12}	2.10E-2	2.60E-4	0.58

Table 6: Uncertainty information for neutronic parameters in a representative segment and branch.

seen in Table 6. These p-values are obtained for segment 14, which is the most common segment in the core. The chosen branch is a representative branch in the normal operation range and corresponds to a fuel temperature of 853.50 K, moderator temperature of 561.40 K and 0.73511 g/cm³ as moderator density. The hypothesis of normality cannot be rejected at a significance level of 5% for all but D_1 responses. However, response D_1 can be considered that follows a quasi-normal distribution. Response distributions are expected to change with burn-up and further studies are needed to understand these variations.

With *Uncertainty Quantification* (UQ) a broad statistical information is obtained (averages, standard deviations, confidence intervals, kurtosis, skewness, etc). Again, this information is obtained for the main homogenized cross sections, feedback parameter combination and segment in core.

5.2. Core level

In the second step, a neutronic library is generated and used to run a steady state simulation with PARCS. the MATLAB code TXT2NTAB is used to generate appropriate neutronic libraries. Besides, PARCS source code is modified to perturb the main cross sections with perturbation factors generated with DAKOTA 6.3 statistical tool. Finally, the uncertainty propagated is reflected in PARCS output parameters (multiplication factor $-k_{\text{eff}}-$, axial power peak $-P_z-$ and peak node location $-N_z-$).

Cross section uncertainty is propagated through PARCS and DAKOTA. As in the lattice model, 1000 sample cases are run. For the purpose of this study, 1000 runs is enough to converge the output statistics. PARCS is not programmed to run different samples and, therefore, the user must run as many cases as desired externally to PARCS. The thermal-hydraulic conditions are feed to PARCS as 3D radial maps, specifically fuel temperature between 900 and 1200 K and moderator density between 100 and 700 kg/m³.

Table 7 contains different statistical information for PARCS responses. The average and standard deviations are shown

	Average	Std. Dev.	p-value
k_{eff}	$1.002 \pm 3.91\text{E-}5$	$6.30\text{E-}4 \pm 2.89\text{E-}5$	0.83
P_z	3.390 ± 0.032	0.516 ± 0.024	~ 0.0
N_z	5.930 ± 0.093	1.500 ± 0.069	~ 0.0

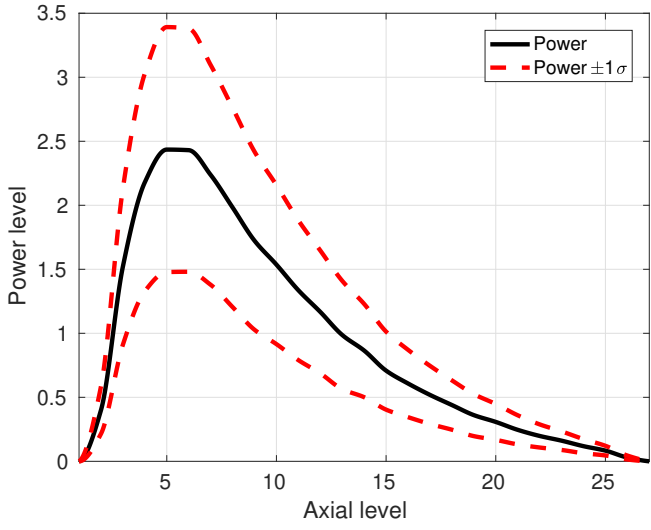
Table 7: Uncertainty information resulting from a global SA

with their confidence interval at 95% level. It is seen that the peak node location has its average value at almost node 6 and a standard deviation of about 1.5. Hence, there is a large chance for the power peak to be located between nodes 4 and 7 –as its histogram shows. This explains why the standard deviation of the axial power profile, Figure 12a, is so wide around the power peak (dashed-red lines). Figure 12b and Figure 12c represents the normalized average radial power profile and its standard deviation. The power peak value in Table 7 is higher than in Figure 12a because they do not represent the same thing. The parameter in Table 7 is the average maximum power regardless of the node location –most probably located between nodes 4 and 7–, whereas the black line in Figure 12a is the average of all axial power profiles –where node location is important–. In both cases the average is performed over the 1000 samples. The key is that the power peak is not always in the same node. Thus, it explains why the power peak in Figure 12a is smaller compared to the value in Table 7, and its standard deviation higher.

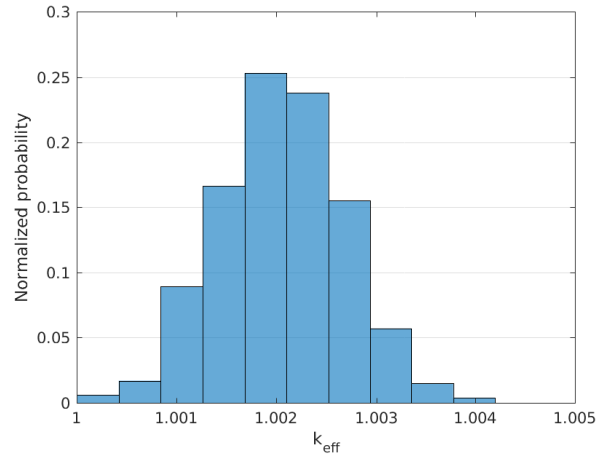
Figure 13 shows the main statistical results obtained for the k_{eff} response in PARCS. It contains its histogram and *Cumulative Distribution Function* (CDF) compared with the standard normal CDF –obtained using the same average and standard deviation. Figure 13c shows the PRCCs for the same response. The Lilliefors test for normality in Table 7 shows that k_{eff} comes from a standard normal distribution. While P_z and N_z do not come from a standard normal distribution.

The *Sensitivity Analysis* (SA) shows that the most sensitive parameters are $\nu\Sigma_{f2}$ and Σ_{a1} , see PRCC plot in Figure 13c. Nonetheless, the PRCC must be studied with caution, especially if there is a large number of input parameters. PRCC is the sensitivity fraction apportioned by an input parameter to an output parameter. Therefore, if one group of input parameters is highly sensitive, the sensitivity fraction apportioned by other input parameters is partially hidden. In this case, the sensitivity apportioned by the homogenized cross sections in neutronic composition 28 and up to composition 33 is high –see Figure 13c where all top ten sensitivity output parameters belong to these neutronic composition range–, thus the sensitivity of homogenized cross sections in other neutronic compositions is relatively low. This effect can be seen in the left plot of Figure 14, where the cumulative PRCC is shown for each segment. The cumulative PRCC is calculated as the normalized sum of all homogenized cross section PRCC belonging to a specific segment, see Eq 7. Thus, the result is the sensitivity fraction apportioned by homogenized cross section in each segment. The cumulative PRCC for each homogenized cross section is also

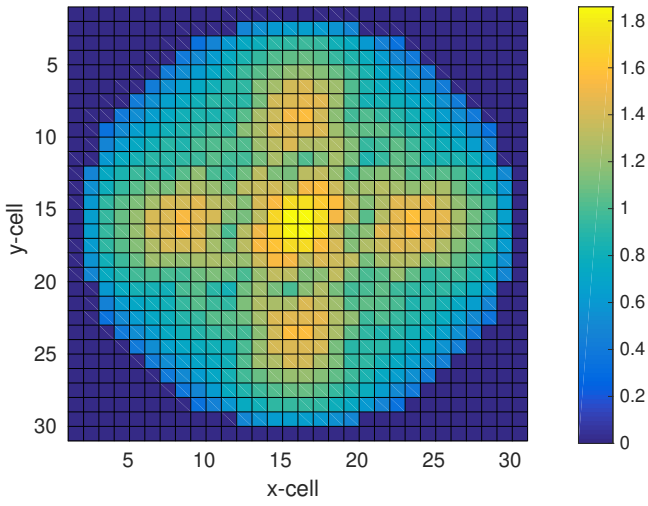
null hypothesis (normality). A larger p-value indicates weak evidence against the null hypothesis, meaning that the test failed to reject the null hypothesis.



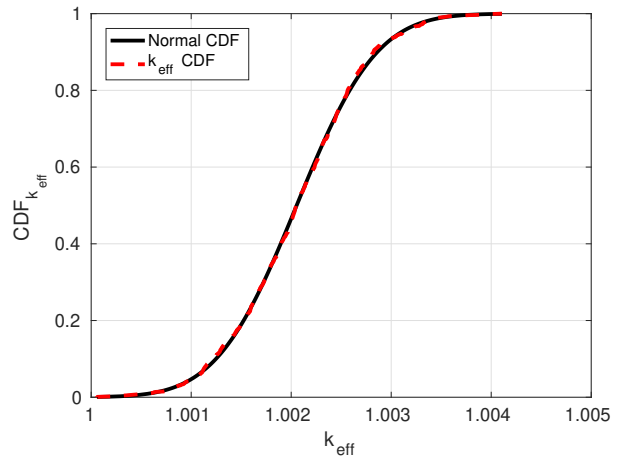
(a) Axial power profile.



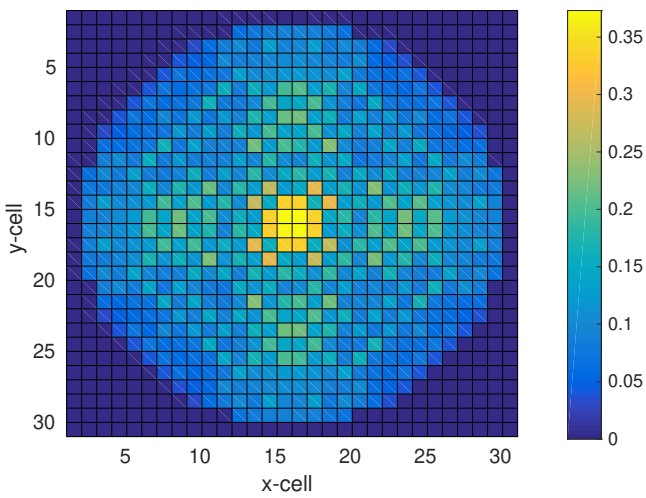
(a) Histogram.



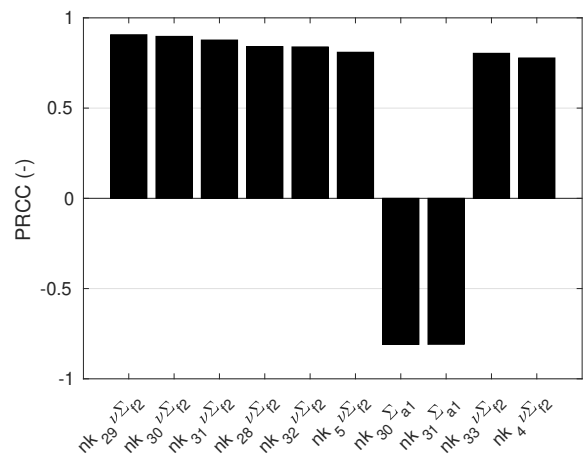
(b) Average collapsed radial power profile.



(b) Cumulative distribution function.



(c) Standard deviation of the collapsed radial power profile.



(c) Partial rank correlation coefficients.

Figure 13: Results for k_{eff} response.

Figure 12: Normalized power profiles

calculated, it is the normalized sum of a specific homogenized cross section PRCC over all segments, see Eq 8. Thus, the result is the sensitivity fraction apportioned by a specific homogenized cross section over the whole core. The result is shown in the right plot of Figure 14.

$$PRCC_{cum}^S = \frac{\sum_{i \in S} |PRCC_i|}{\sum_i |PRCC_i|} \quad (7)$$

$$PRCC_{cum}^X = \frac{\sum_{i \in X} |PRCC_i|}{\sum_i |PRCC_i|} \quad (8)$$

Where

i : input parameter index,

S : segment, and

X : homogenized cross section.

The conclusions from Figure 14 are that the most sensitive homogenized cross sections –for the three considered responses– are those belonging to segment 14 (neutronic compositions from 27 to 49). Information in Figure 6 shows that segment 14 comprises the central nodes in fuel type 8 (from node 3 to 25). Looking at the fuel type distribution of Figure 4, it is easy to understand why the responses are so sensitive to segment 14. Fuel type 8 is used over a great fraction of the radial mapping in this BWR reactor. The second most sensitive segment is segment 13 –according to the left plot of Figure 14–, while reflector segments (1, 2 and 3) and extreme fuel segments (10 and 15) have the lowest sensitivity towards all responses. The most sensitive homogenized cross sections –according to the right plot of Figure 14– for all responses is $\nu\Sigma_{f2}$. This is followed by Σ_{a1} for the k_{eff} response and $\nu\Sigma_{f1}$ for responses P_z and N_z . The diffusion coefficient –both energy groups– has the lowest sensitivity towards the k_{eff} . The other homogenized cross sections have similar sensitivity for responses P_z and N_z .

5.2.1. Analysis by segment

In order to distinguish the most sensitive homogenized cross sections for other segments, the U&S analysis is also performed by segments. Therefore, for each U&S analysis, only the homogenized cross sections belonging to a specific segment are considered as input parameters. Same responses are considered. This analysis is performed for segment 13, this is the second most sensitive segment towards the main responses (see left plot in Figure 14). It is seen that the most sensitive homogenized cross section is, again, $\nu\Sigma_{f2}$. However, now its sensitivity towards P_z and N_z is considerably increased. This is followed by Σ_{a1} for the k_{eff} response and $\nu\Sigma_{f1}$ for responses P_z and N_z . Regarding the other homogenized cross sections, the same conclusions found in the global SA can be applied here.

Table 8 shows the main statistics when only neutronic parameters in segment 13 are perturbed. Comparing the statistics

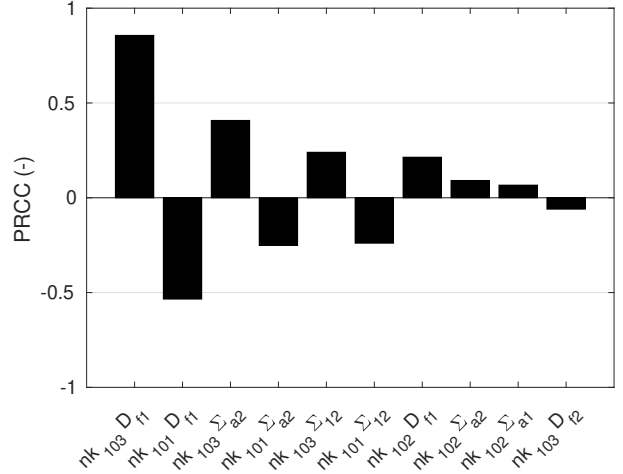


Figure 15: PRCC towards P_z when only neutronic parameters in reflector segments are perturbed.

with the ones obtained in the global SA –Table 7–, it is seen that the standard deviations and their confidence intervals are reduced. In case of k_{eff} and P_z , the reduction is almost one half. The same is observed with the average confidence interval. The Lilliefors test for normality shows that k_{eff} and P_z come from a standard normal distribution. While N_z does not come from a standard normal distribution. The main difference, in comparison with the global SA, is seen in the normality of response P_z .

In order to see the sensitivity of reflector zones, another SA is performed where only homogenized cross sections of reflector compositions are perturbed. In Figure 15 the most sensitive homogenized cross sections are seen for response P_z . The most sensitive reflector composition –for both responses– is composition 103 (radial reflector), followed by composition 101 (bottom reflector). The homogenized cross sections for reflector compositions are almost insensitive towards the node peak location. The most sensitive homogenized cross section is D_{f1} followed by Σ_{a2} .

6. Conclusions

This work presents the main results obtained while testing a new methodology –developed at Universitat Politècnica de València– to propagate the uncertainty of neutronic parameters. This methodology covers the main phases of the benchmark released by the expert group on *Uncertainty Analysis in Modeling of Light Water Reactors* (UAM-LWR). To achieve this purpose several models are developed. A lattice physics model is developed with SCALE/NEWT and validated with a code-to-code comparison with CASMO-4. Besides, TXT2NTAB MATLAB program is developed to obtain neutronic libraries in NEMTAB format out of TRITON/NEWT transport code results.

The most straightforward procedure to propagate the uncertainty information between codes is the generation of n

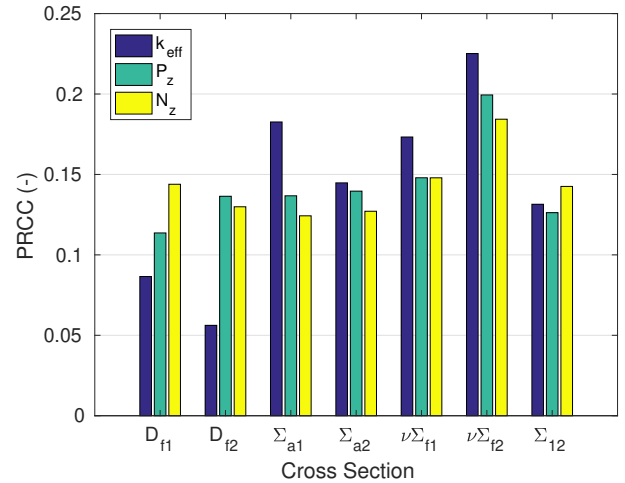
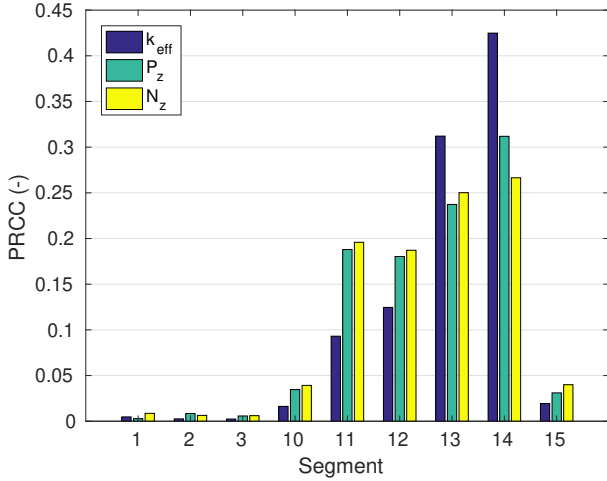


Figure 14: Cumulative PRCC by segment (left) and by cross section (right) for the global SA.

	Average	Std. Dev.	p-value
k_{eff}	$1.002 \pm 1.98\text{E-}5$	$3.19\text{E-}4 \pm 1.46\text{E-}5$	0.33
P_z	2.931 ± 0.018	0.290 ± 0.013	0.66
N_z	5.760 ± 0.069	1.107 ± 0.051	~ 0.0

Table 8: Uncertainty information when only neutronic parameters in segment 13 are perturbed.

“low-fidelity” covariance libraries or what segment model should be simulated in more detail. Another phenomena to take into account is that if one segment is highly sensitive, homogenized cross sections belonging to other segments are partially hidden in the global SA. To disclose the sensitivity of homogenized cross sections belonging to less sensitive segments, another SA performed over a specific segment can be done.

neutronic libraries that are used to run the core physics code n times. An alternative option is presented in this work. Only two neutronic libraries are generated, one with the average responses and the other with their standard deviations. Then, the standard deviation and a matrix of perturbation factors are used to perturb the neutronic parameters feed into the core physics code. Nonetheless, normality for these parameters must be assumed. This assumption must be checked at the end with a normality test.

The UQ performed shows that the accuracy of neutronic data propagation –at lattice and core level– depends on the number of samples (perturbations). In this work, the maximum number of samples allowed by SAMPLER (1000) is used, although it is seen that output variables converge at around 300 samples. A thousand samples is also used for PARCS propagation. Moreover, it is seen that the homogenized neutronic parameters under study follow a normal –or quasi-normal for D_1 – distribution. In this case a fresh case is used, therefore, the normality of this parameters must be assessed in future studies for cases with a certain degree of burn-up. Besides, for the core physics code, the multiplication factor also follows a normal distribution.

The SA shows that the most sensitive homogenized cross section is $\nu\Sigma_{f2}$. Depending on the neutronic parameter studied, it is followed by Σ_{a1} or $\nu\Sigma_{f1}$. It is also possible to determine which is the most sensitive segment in the core. This could lead to define what could be the next steps to update the current

A long simulation time and effort was needed to perform this work due to the high number of samples chosen. The bottle neck is in the lattice code (56 branches and 1000 perturbations) that takes 22 days using around 150 processors and 150 Gb of memory. The total process –lattice and core– is around 25 days. Due to this computational cost, it was decided to model all fuel assemblies as fresh. Another simplification is the lack of thermal-hydraulic parameter propagation since there is not thermal-hydraulic coupling. However, a parallel work is done to propagate the thermal-hydraulic parameters in a PWR core [1] (without neutronic propagation). It is known that these simplifications could lead to possible different uncertainties in a more realistic core. Therefore, in the future, this work will be repeated with SCALE/Polaris, the new deterministic 2D lattice physics code included in SCALE and faster than NEWT. The reduction of the sample size in the lattice model is another option to reduce the computational cost.

Acknowledgement

The authors of this work thank IBERINCO (Iberdrola Ingeniera y Construccin, S. A.) for the shared data which made possible the validation of the lattice physics model. Moreover, this work was possible thanks to the UAM-LWR benchmark release, thanks to its organizers who requested the development of TXT2NTAB MATLAB program. Finally, the authors sincerely thank to the Ministerio de Economa, Industria y Competitividad and the “Plan Nacional de I+D+i” for funding the projects NUC-MULTPHYS ENE2012-34585 and ENE2017-89029-P.

References

- [1] C. Mesado, R. Miró, G. Verdú, Application Case for Phase iii of UAM-LWR Benchmark: Uncertainty Propagation of Thermal-Hydraulic Macroscopic Parameters, Nuclear Engineering and Technology doi : 10.1016/j.net.2020.01.010.
- [2] K. Ivanov, M. Avramova, S. Kamerow, I. Kodeli, E. Sartori, E. Ivanov, O. Cabellos, Benchmarks for Uncertainty Analysis in Modelling (UAM) for the Design, Operation and Safety Analysis of LWRs-Volume I: Specification and Support Data for Neutronics Cases (Phase I), Tech. rep., Organisation for Economic Co-Operation and Development, Nuclear Energy Agency-OECD/NEA (2013).
- [3] D. Rochman, O. Leray, M. Hursin, H. Ferroukhi, A. Vasiliev, A. Aures, F. Bostelmann, W. Zwermann, O. Cabellos, C. J. Diez, et al., Nuclear Data Uncertainties for Typical LWR Fuel Assemblies and a Simple Reactor Core, Nuclear Data Sheets 139 (2017) 1–76.
- [4] O. Leray, H. Ferroukhi, M. Hursin, A. Vasiliev, D. Rochman, Methodology for Core Analyses with Nuclear Data Uncertainty Quantification and Application to Swiss PWR Operated Cycles, Annals of Nuclear Energy 110 (2017) 547–559. doi : 10.1016/j.anucene.2017.07.006.
- [5] M. Avramova, K. Ivanov, B. Krzykacz-Hausmann, K. Velkov, A. Pautz, Y. Perin, Uncertainty analysis of COBRA-TF void distribution predictions for the OECD/NRC BFBT Benchmark, in: Proceedings of the International Conference on Advances in Mathematics, Computational Methods, and Reactor Physics (M&C09), 2009.
- [6] D. A. Rochman, E. Bauge, A. Vasiliev, H. Ferroukhi, G. Perret, Nuclear Data Correlation Between Different Isotopes via Integral Information, EPJ Nuclear Sciences & Technologies 4 (2018) 7.
- [7] C. Mesado, A. Soler, T. Barrachina, R. Miró, J. García-Díaz, R. Macián-Juan, G. Verdú, Uncertainty and Sensitivity of Neutron Kinetic Parameters in the Dynamic Response of a PWR Rod Ejection Accident Coupled Simulation, Science and Technology of Nuclear Installations, 2012 doi : 10.1155/2012/625878.
- [8] A. Hernández-Solís, Uncertainty and Sensitivity Analysis Applied to LWR Neutronic and Thermal-Hydraulic Calculations, Ph.D. thesis, Chalmers University of Technology (2012).
- [9] G. Strydom, Uncertainty and Sensitivity Analyses of a Pebble Bed HTGR Loss of Cooling Event, Science and Technology of Nuclear Installations, 2013 doi : 10.1155/2013/426356.
- [10] S. Wilks, Determination of sample sizes for setting tolerance limits, The Annals of Mathematical Statistics 12 (1) (1941) 91–96.
- [11] S. Wilks, Statistical prediction with special reference to the problem of tolerance limits, The annals of mathematical statistics 13 (4) (1942) 400–409.
- [12] R. Macin-Juan, W. Tietsch, F. Sassen, Proposal for the Development and Implementation of an Uncertainty and Sensitivity Analysis Module in SNAP, US NRC NUREG/IA-0407, 2012.
- [13] I. Hong, D. Oh, I. Kim, Generic Application of Wilks’ Tolerance Limit Evaluation Approach to Nuclear Safety, 2013.
- [14] I. Hong, A. Connolly, Generalized Tolerance Limit Evaluation Method to Determine Statistically Meaningful Minimum Code Simulations, in: 16th International Conference on Nuclear Engineering, American Society of Mechanical Engineers, 2008, pp. 653–660.
- [15] L. Pal, M. Makai, Remarks on Statistical Aspects of Safety Analysis of Complex Systems, ArXiv Preprint Physics/0308086, 2002.
- [16] A. Guba, M. Makai, L. Pál, Statistical Aspects of Best Estimate Method I, Reliability Engineering & System Safety 80 (3) (2003) 217–232.
- [17] D. C. Wicaksono, Bayesian Uncertainty Quantification of Physical Models in Thermal-Hydraulics System Codes, Ph.D. thesis, Lausanne (2018). doi : 10.5075/epfl-thesis-8426. URL <http://infoscience.epfl.ch/record/253113>
- [18] M. Perez, F. Reventos, L. Batet, A. Guba, I. Tóth, T. Mieusset, P. Bazin, A. De Crécy, S. Borisov, T. Skorek, et al., Uncertainty and Sensitivity Analysis of a LBLOCA in a PWR Nuclear Power Plant: Results of the Phase V of the BEMUSE Programme, Nuclear Engineering and Design 241 (10) (2011) 4206–4222.
- [19] W. Conover, Practical nonparametric statistics, third edition, 3rd Edition, John Wiley & Sons, Inc, 1999.
- [20] D. Cruz, D. Rochman, A. Koning, Propagation of Nuclear Data Uncertainty for a Control Rod Ejection Accident Using the Total Monte-Carlo Method, in: Proceedings of the International Conference on Physics of Reactors (PHYSOR 2014), Japan Atomic Energy Agency, 2014.
- [21] C. Mesado, Uncertainty Quantification and Sensitivity Analysis for Cross Sections and Thermohydraulic Parameters in Lattice and Core Physics Codes. Methodology for Cross Section Library Generation and Application to PWR and BWR, Ph.D. thesis, Universitat Politècnica de València (2017). URL <http://hdl.handle.net/10251/86167>
- [22] B. Ade, SCALE/TRITON Primer: A Primer for Light Water Reactor Lattice Physics Calculations, Tech. rep., Oak Ridge National Laboratory (ORNL) (2012).
- [23] D. Wang, B. Ade, A. Ward, Cross Section Generation Guidelines for TRACE-PARCS, Tech. rep., Oak Ridge National Laboratory (ORNL) (2013).
- [24] A. Labarile, C. Mesado, R. Miró, G. Verdú, Cross-sections Generation using TXT2NTAB Code for Uncertainty Propagation with Burnup Dependence, Nuclear Technology, 2019.
- [25] A. Yankov, B. Collins, M. Klein, M. A. Jessee, W. Zwermann, K. Velkov, A. Pautz, T. Downar, A Two-Step Approach to Uncertainty Quantification of Core Simulators, Science and Technology of Nuclear Installations 2012. doi : 10.1155/2012/767096.